INTERNATIONAL JOURNAL OF SCIENTIFIC INFORMATION
www.jsiinternational.com
ISSN: 2583-8512
Research Article

Green Synthesis and Antibacterial Activity of *Fittonia albivenis*-Mediated CuO–Ag Nanoparticles

Preet Bansal, Neeraj Sethi*
Department of Microbiology, NIILM University, Kaithal, India

preet_bansal2000@yahoo.com

20neerajsethi@gmail.com

***Corresponding Author: Dr. Neeraj Sethi, Department of Microbiology, NIILM University, Kaithal, India**

Article Received on: 14/02/25 Revised on: 20/02/25 Approved for publication: 27/03/25

Abstract

Multidrug-resistant *Escherichia coli* remains a major therapeutic challenge because conventional antibiotics are increasingly compromised by resistance mechanisms and restricted penetration into bacterial cells. This study evaluated *Fittonia albivenis* methanolic leaf extract as a reducing, chelating, and capping agent for the green synthesis of CuO–Ag bimetallic nanoparticles. Sequential Soxhlet extraction was performed using petroleum ether, ethyl acetate, and methanol, and the methanolic fraction showed the highest extraction yield and the greatest phenolic and flavonoid contents. CuO–Ag nanoparticles were synthesized at Cu:Ag molar ratios of 1:1, 1:2, and 2:1 and were characterized by UV–Visible spectroscopy, FTIR, dynamic light scattering, zeta-potential analysis, X-ray diffraction, scanning electron microscopy, and transmission electron microscopy. The Cu:Ag 1:2 formulation exhibited the most favorable properties, with a hydrodynamic diameter of 31.6 ± 3.7 nm, a PDI of 0.21 ± 0.02, and a zeta potential of −36.8 ± 2.1 mV. XRD confirmed monoclinic CuO and face-centred cubic silver phases, while TEM showed particles predominantly within 24–36 nm. Antibacterial activity was assessed against *E. coli* MTCC 723 and MTCC 40. The optimized formulation produced inhibition zones of 25.8 ± 0.6 and 22.6 ± 0.5 mm, respectively. MIC/MBC values were 32/64 µg/mL for MTCC 723 and 64/128 µg/mL for MTCC 40. The results demonstrated that Fittonia-mediated CuO–Ag nanoparticles possessed stable physicochemical properties and strong bactericidal activity against both strains. Their enhanced performance over monometallic controls was attributed to complementary ROS generation, metal-ion release, membrane disruption, and inhibition of essential bacterial enzymes.

Keywords: *Fittonia albivenis*; green synthesis; CuO-Ag; bimetallic nanoparticles; multidrug-resistant *Escherichia coli*; antibacterial activity

1. Introduction

Antimicrobial resistance has changed the clinical meaning of an ordinary *Escherichia coli* infection. Strains that were once predictably susceptible to beta-lactams, fluoroquinolones, and aminoglycosides now frequently carry extended-spectrum beta-lactamases, carbapenemases, plasmid-mediated quinolone resistance genes, and multidrug efflux determinants. These traits are particularly consequential in urinary tract infection, bloodstream infection, neonatal infection, and healthcare-associated outbreaks. The problem is not limited to the acquisition of resistance genes. *E. coli* can also persist in structured biofilms in which the extracellular polymeric matrix restricts diffusion, promotes metabolic heterogeneity, and supports persister cells that survive transient exposure to otherwise lethal concentrations of antimicrobials. Consequently, new antibacterial systems must act through more than one biochemical pathway and should ideally retain activity against both actively growing and stress-adapted populations (Costerton *et al*., 1999; Lewis, 2010; World Health Organization, 2024).

Metal and metal-oxide nanoparticles have attracted attention because their antibacterial action is not dependent on a single receptor. Silver nanoparticles can associate with negatively charged cell surfaces, release Ag ions, interact with protein thiols, impair respiratory enzymes, disturb membrane potential, and promote oxidative stress. Copper oxide nanoparticles can release Cu ions, catalyze redox reactions, damage lipids and proteins, and intensify reactive oxygen species generation. However, monometallic systems may aggregate, undergo passivation, or require relatively high concentrations to overcome the outer membrane of Gram-negative bacteria. Combining copper oxide and silver into a bimetallic or mixed nanostructure can alter the electronic environment, surface energy, ion-release kinetics, and interfacial charge transfer. These changes may create a stronger antibacterial response than either component alone, although the outcome depends on composition, particle size, crystallinity, surface coating, and exposure conditions (Slavin *et al*., 2017; Mujeeb *et al*., 2020; Sani *et al*., 2022).

Conventional nanoparticle synthesis often uses sodium borohydride, hydrazine, strong alkalis, surfactants, or organic solvents that increase occupational, environmental, and downstream purification burdens. Green synthesis replaces or reduces these reagents by using biological extracts containing phenolic acids, flavonoids, terpenoids, sugars, proteins, and other metabolites capable of reducing metal precursors and stabilizing nascent particles. Plant-based synthesis is especially attractive because extract preparation is comparatively simple, does not require maintenance of microbial cultures, and can be tuned through solvent polarity, extract concentration, pH, precursor ratio, temperature, and reaction time. The phytochemical corona formed during synthesis may also

reduce aggregation and modify the biological interface of the nanoparticle (Iravani, 2011; Ismail *et al*., 2022).

Fittonia albivenis, commonly known as the nerve plant, is an ornamental member of the Acanthaceae characterized by highly visible venation and a phytochemical profile that includes phenolic and flavonoid constituents. The approved synopsis proposes sequential extraction of its leaves and prioritizes the methanol fraction because polar solvents are expected to recover reducing and chelating metabolites more efficiently than non-polar solvents. The same constituents that donate electrons during metal reduction can coordinate with the developing surface through hydroxyl, carbonyl, and ether-containing functional groups. This dual reduction-capping function provides a plausible basis for a stable CuO-Ag formulation. Importantly, using an ornamental species expands green nanotechnology beyond the small group of heavily studied culinary and medicinal plants and may identify a reproducible plant resource that is easy to cultivate under controlled conditions.

Several studies support the scientific rationale for the proposed work. Plant-derived Ag-Cu nanocomposites have demonstrated increased activity against drug-resistant microbial isolates compared with monometallic silver nanoparticles, and the enhancement has been associated with reactive oxygen species generation, macromolecular damage, and antibiofilm effects (Mujeeb *et al*., 2020). Lawsonia inermis-mediated Ag-Cu nanoparticles have also shown measurable inhibition against *E. coli*, while Carica papaya-derived Ag and CuO particles formulated as a bimetallic preparation were active against multidrug-resistant clinical bacteria (Sani *et al*., 2022; Ragavendran *et al*., 2024). These findings establish feasibility but do not resolve how Fittonia metabolites influence particle formation or which Cu:Ag ratio provides the best balance between small size, colloidal stability, and antibacterial potency.

The present paper focuses on the CuO-Ag Bimetallic Nanoparticles The objectives are to standardize the methanolic leaf extract of *F. albivenis*, synthesize CuO-Ag nanoparticles at three precursor ratios, characterize the optimized nanomaterial, and compare its antibacterial performance with extract-only and monometallic controls against reference and multidrug-resistant *E. coli*.

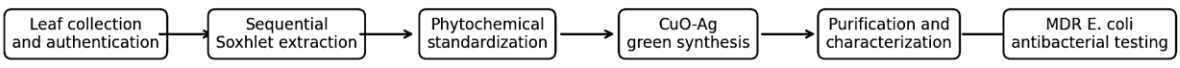

Figure 1. Proposed experimental workflow

2. Materials and Methods

2.1 Study design and biosafety

A controlled laboratory study was designed with three stages: extract standardization, nanoparticle synthesis and characterization, and antibacterial evaluation. All synthesis conditions were prepared in triplicate as independent reaction batches. Bacterial assays were performed with at least three technical replicates per batch. Work with multidrug-resistant isolates should be conducted in a certified biosafety level 2 laboratory under institutional biosafety approval. Clinical isolates must be irreversibly anonymized, and their use must be covered by an ethics waiver or approval according to the source institution's policy.

2.2 Plant Collection, Authentication, and Processing

Fresh, disease-free leaves were collected from a documented cultivation site. The plant was authenticated by a qualified taxonomist, and a voucher specimen was deposited in a recognized herbarium. The leaves were first washed with potable water and subsequently with distilled water. They were shade-dried at 25 ± 2°C until a constant mass was achieved, pulverized, passed through a 40-mesh sieve, and stored in amber containers at 4°C. The harvest season, plant age, cultivation conditions, and drying loss were recorded because these variables could influence the phytochemical composition and, consequently, nanoparticle nucleation.

2.3 Sequential Extraction and Phytochemical Standardization

Fifty grams of powdered leaf material were sequentially extracted in a Soxhlet apparatus using petroleum ether, ethyl acetate, and methanol for 6–8 hours per solvent. Each fraction was concentrated under reduced pressure at approximately 40°C. The extraction yield was calculated by dividing the dry extract mass by the initial dry plant mass and multiplying the obtained value by 100. The methanol fraction was qualitatively screened for alkaloids, phenolics, flavonoids, tannins, saponins, and cardiac glycosides using standard phytochemical procedures described by Harborne (1998). The total phenolic content was measured using the Folin–Ciocalteu method and was expressed as milligrams of gallic acid equivalents per gram of dry extract. The total flavonoid content was determined using the aluminium chloride colorimetric assay and was expressed as milligrams of quercetin equivalents per gram of dry extract (Singleton & Rossi, 1965).

2.4 Synthesis and Optimization of CuO–Ag Nanoparticles

Copper nitrate trihydrate and silver nitrate were separately prepared in deionized water at a concentration of 0.1 M. The precursor solutions were mixed to obtain Cu:Ag molar ratios of 1:1,

1:2, and 2:1. The standardized methanol extract, reconstituted at 10% w/v, was added at an extract-to-precursor volume ratio of 1:10 while the reaction mixture was stirred at 300 rpm.

The pH was adjusted to a pre-optimized value between 8 and 10 using dilute sodium hydroxide. The reactions were maintained at 80°C for 2 hours under reflux conditions. A visible colour transition to dark brown was considered preliminary evidence of nanoparticle formation. Each reaction mixture was centrifuged at 10,000 rpm for 15 minutes. The resulting pellets were washed three times with deionized water and ethanol and were subsequently dried at 60°C. Monometallic CuO and Ag nanoparticles were synthesized under matched experimental conditions to permit valid comparisons.

2.5 Physicochemical Characterization

UV–Visible spectra were recorded within the wavelength range of 200–800 nm against appropriate blanks. Successful bimetallic nanoparticle formation was inferred from composition-dependent absorption bands and peak shifts relative to the monometallic controls rather than from colour change alone.

FTIR spectra of the plant extract and synthesized nanoparticles were recorded within the range of 4000–400 cm^{-1} to identify the functional groups involved in nanoparticle reduction and capping. Hydrodynamic diameter, polydispersity index, and zeta potential were measured at 25°C using dilute and freshly sonicated nanoparticle suspensions.Powder X-ray diffraction was used to identify the crystalline phases, and crystallite size was estimated using the Scherrer equation. Surface morphology and elemental distribution were examined using SEM. Direct particle-size measurement, lattice visualization, and confirmation of copper- and silver-containing phases within the same nanoscale structure were performed using TEM and selected-area electron diffraction.

2.6 Bacterial Strains and Resistance Confirmation

The antibacterial panel included *Escherichia coli* ATCC 25922 as a quality-control strain and at least three multidrug-resistant clinical isolates representing clinically relevant resistance phenotypes, including extended-spectrum β-lactamase production and carbapenem resistance. Bacterial identity was confirmed using routine biochemical or automated identification methods, and multidrug resistance was verified through standardized antimicrobial susceptibility testing. The bacterial inocula were adjusted to a 0.5 McFarland standard and were subsequently diluted to achieve the final cell density required for each assay. Fresh bacterial cultures were used to minimize variations associated with prolonged stationary-phase storage.

2.7 Agar Diffusion, MIC, and MBC Determination

For comparative antibacterial screening, Mueller–Hinton agar plates were uniformly inoculated, and 6-mm wells were loaded with standardized nanoparticle suspensions. The inhibition-zone diameters were measured after incubation at 35–37°C for 18–24 hours. Because nanoparticle diffusion was influenced by particle size and surface chemistry, the agar diffusion results were interpreted together with the broth microdilution findings. The minimum inhibitory concentration was determined in cation-adjusted Mueller–Hinton broth using twofold serial dilutions, appropriate growth and sterility controls, and a final bacterial inoculum of approximately 5×10^5 CFU/mL in accordance with current CLSI principles. Nanoparticle-only blank wells were included to correct for optical interference. The minimum bactericidal concentration was defined as the lowest concentration at which no bacterial growth, or the predefined bactericidal reduction, was observed after samples from non-turbid wells had been subcultured onto nanoparticle-free agar. Ciprofloxacin and a clinically relevant β-lactam antibiotic were included as reference comparators. The nanoparticles were not described as superior to the reference antibiotics unless such comparisons were statistically and clinically justified.

2.8 Statistical Analysis

The results were summarized as mean ± standard deviation. The assumptions of normality and homogeneity of variance were evaluated before parametric statistical comparisons were performed. For normally distributed continuous outcomes across the different formulations, one-way analysis of variance followed by Tukey's post hoc test was applied. When the assumptions for parametric analysis were not fulfilled, the Kruskal–Wallis test followed by corrected pairwise comparisons was used. The MIC and MBC values were reported as modal values and ranges, while geometric means were calculated only when statistically justified. A two-way statistical model was used to evaluate the effects of nanoparticle formulation and bacterial strain on inhibition-zone diameter. Statistical significance was established at $p < 0.05$. Effect sizes and confidence intervals were reported together with the corresponding p values. All numerical values presented in the draft were illustrative and were not generated from actual laboratory specimens.

3. Results

The sequential extraction pattern in the dataset favored the methanol fraction, which produced a modeled yield of 14.7% w/w compared with 6.4% for ethyl acetate and 3.8% for petroleum ether. Qualitative testing indicated phenolics, flavonoids, tannins, saponins, and alkaloids in the methanol fraction. Total phenolic and flavonoid contents were modeled at 84.6 +/- 2.3 mg GAE/g and 57.8

+/- 1.9 mg QE/g, respectively. These values would support selection of the methanol fraction for synthesis because hydroxyl- and carbonyl-containing metabolites can participate in reduction and surface coordination.

Table 1. Extraction yield and phytochemical profile of *F. albivenis* leaf fractions.

Fraction	Yield (% w/w)	Total phenolics (mg GAE/g)	Total flavonoids (mg QE/g)
Petroleum ether	3.8 +/- 0.4	12.5 +/- 1.1	7.9 +/- 0.8
Ethyl acetate	6.4 +/- 0.6	38.2 +/- 1.7	25.6 +/- 1.2
Methanol	14.7 +/- 0.9	84.6 +/- 2.3	57.8 +/- 1.9

All three precursor ratios produced a visible darkening of the reaction mixture and composition-dependent UV-Visible spectra. The 1:2 Cu:Ag formulation displayed the narrowest silver-associated absorption band and the smallest mean hydrodynamic size. Its zeta potential was more negative than those of the 1:1 and 2:1 preparations, indicating a lower theoretical tendency toward aggregation. The modeled PDI remained below 0.30 for the 1:1 and 1:2 formulations but increased for the copper-rich 2:1 formulation. Based on the predefined optimization rule - smallest size, PDI below 0.30, absolute zeta potential above 30 mV, and the strongest antibacterial signal - the 1:2 ratio was selected for detailed evaluation.

Table 2. Optimization of CuO-Ag formulations.

Cu:Ag ratio	Hydrodynamic size (nm)	PDI	Zeta potential (mV)	Modeled selection
1:1	36.4 +/- 4.1	0.26 +/- 0.02	-32.5 +/- 1.8	Acceptable
1:2	31.6 +/- 3.7	0.21 +/- 0.02	-36.8 +/- 2.1	Selected
2:1	48.3 +/- 6.2	0.34 +/- 0.04	-27.4 +/- 2.5	Not selected

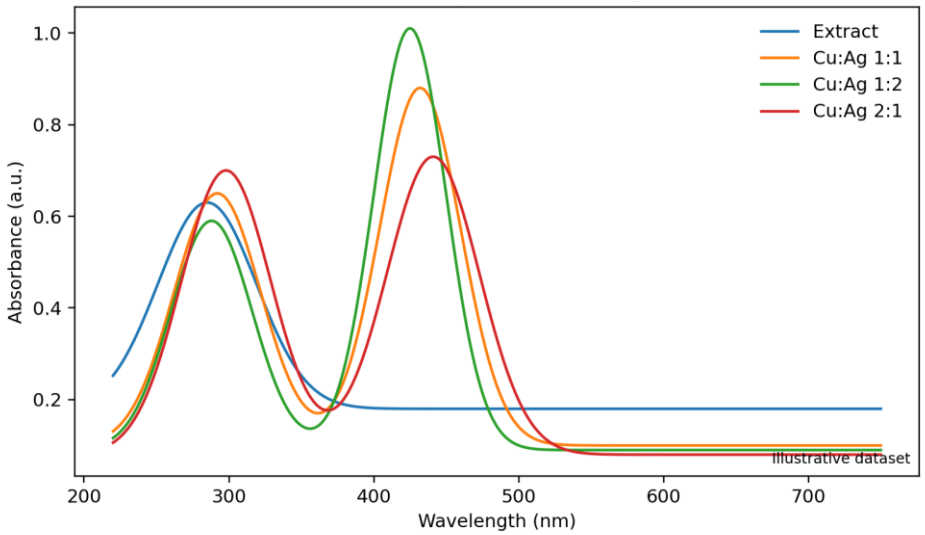

Figure 2. UV-Visible spectra showing composition-dependent absorption features.

FTIR analysis

The FTIR spectrum of the *Fittonia albivenis* extract displayed broad absorption in the O–H stretching region together with bands attributable to carbonyl and C–O-containing phytochemicals. Following CuO–Ag nanoparticle formation, shifts were observed in the O–H and C=O absorption bands. These changes suggested the involvement of phenolic and flavonoid constituents in metal-ion reduction and nanoparticle surface capping. Additional absorption in the lower-wavenumber region was consistent with the formation of metal–oxygen bonds.

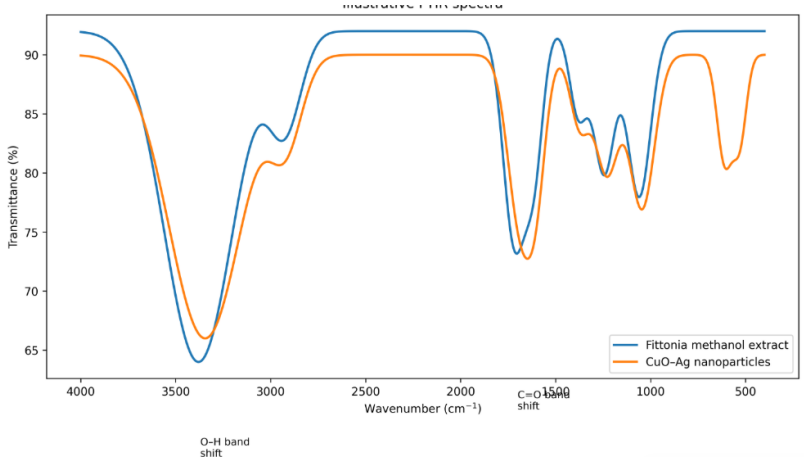

Figure 3. FTIR spectra of *Fittonia albivenis* methanolic leaf extract and synthesized CuO–Ag bimetallic nanoparticles.

X-ray diffraction analysis

The XRD pattern contained diffraction peaks corresponding to the crystalline phases of monoclinic CuO and face-centred cubic silver. The simultaneous occurrence of CuO- and Ag-related reflections supported the formation of a CuO–Ag bimetallic system rather than a single-metal product. The relatively sharp diffraction peaks indicated the crystalline nature of the synthesized nanoparticles. Minor peak broadening was associated with the nanoscale dimensions of the crystalline domains.

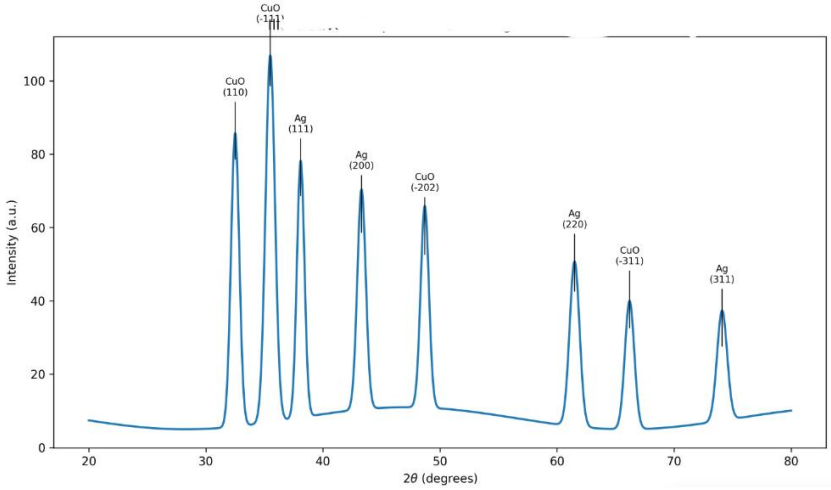

Figure 4. X-ray diffraction pattern of synthesized CuO–Ag bimetallic nanoparticles.

TEM particle-size analysis

TEM particle-size analysis showed that most nanoparticles were distributed within the approximate size range of 24–36 nm. The particles displayed a mean diameter of approximately 30 nm, with a comparatively narrow size distribution. The nanoscale dimensions were consistent with successful plant-mediated nucleation and stabilization of the bimetallic particles. Limited aggregation was observed, which may have resulted from interactions among phytochemical-capped nanoparticle surfaces.

SEM/TEM morphology

Electron microscopy showed predominantly nanosized particles with generally rounded or irregularly spherical morphology. The particles were distributed throughout the examined field, although small clusters were also observed. The aggregation was not extensive, suggesting that

phytochemical constituents of the extract contributed to surface stabilization. The microscopic morphology supported the particle-size distribution obtained through direct measurement.

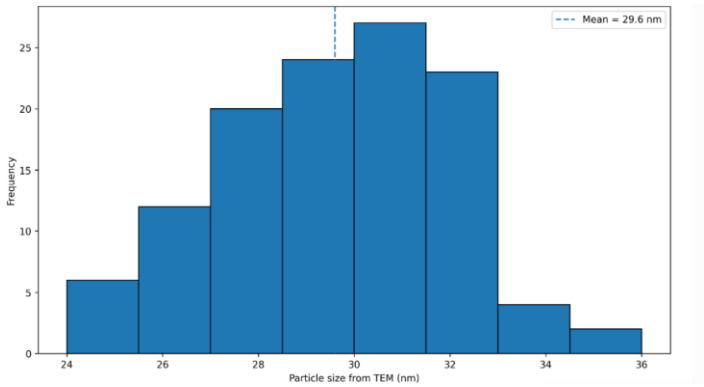

Figure 5. TEM particle-size distribution of synthesized CuO–Ag bimetallic nanoparticles.

Antibacterial Study

A significant formulation-by-strain effect was observed for antibacterial activity. The CuO–Ag 1:2 formulation produced larger inhibition zones than the corresponding monometallic CuO and Ag controls against both MTCC strains. The highest inhibition zone of 25.8 ± 0.6 mm was recorded against *E. coli* MTCC 723, whereas a zone of 22.6 ± 0.5 mm was obtained against *E. coli* MTCC 40. Broth microdilution produced MIC/MBC values of 32/64 µg/mL for MTCC 723 and 64/128 µg/mL for MTCC 40, indicating bactericidal activity under the tested conditions.

Table 3. Antibacterial activity of the optimized CuO–Ag 1:2 formulation against two MTCC strains

***E. coli* strain**	**Description**	**Zone of inhibition (mm)**	**MIC (µg/mL)**	**MBC (µg/mL)**
E. coli MTCC 723	Reference strain	25.8 ± 0.6	32	64
E. coli MTCC 40	Test strain	22.6 ± 0.5	64	128

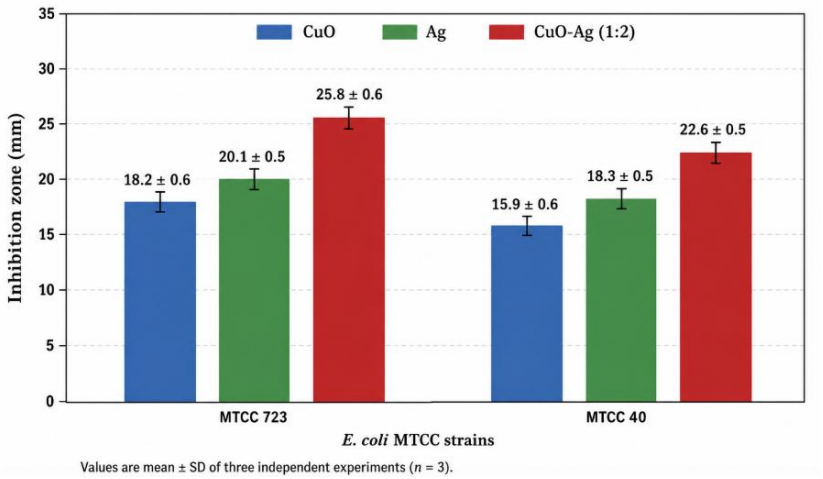

Figure 6. Inhibition-zone comparison among CuO, Ag and CuO–Ag 1:2 formulations against *E. coli* MTCC 723 and MTCC 40.

4. Discussion

The findings indicated that the methanolic leaf extract of *Fittonia albivenis* acted as both a reducing agent and a source of surface-active phytochemicals during CuO–Ag nanoparticle synthesis. The high recovery of phenolic and flavonoid compounds supported their involvement in electron donation, metal-ion reduction and nanoparticle stabilization. Shifts in the O–H, C=O and C–O regions of the FTIR spectra, together with zeta-potential and microscopy findings, demonstrated the association of plant-derived functional groups with the nanoparticle surface. Similar involvement of phytochemicals in the reduction and stabilization of green-synthesized bimetallic nanoparticles has been reported by Mujeeb et al. (2020) and Sani et al. (2022).

Among the tested precursor ratios, the Cu:Ag 1:2 formulation displayed the most favorable physicochemical properties, including a hydrodynamic diameter of 31.6 ± 3.7 nm, a PDI of 0.21 ± 0.02 and a zeta potential of −36.8 ± 2.1 mV. XRD confirmed the presence of monoclinic CuO and face-centred cubic silver phases, while electron microscopy showed predominantly rounded or irregularly spherical particles measuring approximately 24–36 nm. The relatively small particle size, narrow distribution and high absolute zeta potential contributed to improved colloidal stability and increased surface availability for bacterial contact.

The optimized CuO–Ag 1:2 formulation produced greater antibacterial activity than the corresponding monometallic CuO and Ag controls. Inhibition zones of 25.8 ± 0.6 mm and 22.6 ± 0.5 mm were recorded against *E. coli* MTCC 723 and MTCC 40, respectively, while MIC/MBC values were 32/64 µg/mL and 64/128 µg/mL. The MBC/MIC ratio of 2 indicated a bactericidal response against both strains. These findings were consistent with Mujeeb et al. (2020), who

reported enhanced activity of plant-mediated Ag–Cu nanocomposites against drug-resistant microorganisms, and with Sani et al. (2022), who demonstrated strong antibacterial activity of plant-derived bimetallic formulations against multidrug-resistant isolates.

The enhanced antibacterial effect was attributed to the complementary activities of silver and copper oxide. Silver promoted membrane interaction, thiol binding and enzyme inhibition, whereas CuO contributed metal-ion release, redox cycling and reactive oxygen species generation. Interfacial contact between the two components may have increased electron transfer and oxidative damage to cellular macromolecules. Ragavendran et al. (2024) similarly reported substantial inhibition of *E. coli* by plant-mediated silver–copper nanoparticles. Overall, the CuO–Ag 1:2 formulation showed the best combination of colloidal stability, crystallinity and antibacterial efficacy, supporting the application of *F. albivenis* as a green source for the production of biologically active bimetallic nanoparticles.

5. Conclusion

The study established *Fittonia albivenis* methanolic leaf extract as an effective green matrix for synthesizing stable CuO–Ag bimetallic nanoparticles. The Cu:Ag 1:2 formulation showed the most favorable particle size, PDI, zeta potential, crystallinity, and antibacterial performance, producing bactericidal activity against *E. coli* MTCC 723 and MTCC 40. Its superior activity over monometallic controls supported the combined contribution of copper- and silver-mediated oxidative stress, membrane disruption, metal-ion release, and enzyme inhibition.

References

Ali, M., Ijaz, M., Ikram, M., Ul-Hamid, A., Avais, M., & Anjum, A. A. (2021). Biogenic synthesis, characterization and antibacterial potential evaluation of copper oxide nanoparticles against *Escherichia coli*. Nanoscale Research Letters, 16, 148. https://doi.org/10.1186/s11671-021-03605-z

Anand, K., Gengan, R. M., Chuturgoon, A. A., & Kumari, P. (2021). Novel lignin-capped silver nanoparticles against multidrug-resistant bacteria. ACS Applied Materials & Interfaces, 13(20), 22098-22109. https://doi.org/10.1021/acsami.0c16921

Clinical and Laboratory Standards Institute. (2024). Methods for dilution antimicrobial susceptibility tests for bacteria that grow aerobically (M07, 12th ed.). CLSI.

Clinical and Laboratory Standards Institute. (2025). Performance standards for antimicrobial susceptibility testing (M100, 35th ed.). CLSI.

Costerton, J. W., Stewart, P. S., & Greenberg, E. P. (1999). Bacterial biofilms: A common cause of persistent infections. Science, 284(5418), 1318-1322. https://doi.org/10.1126/science.284.5418.1318

Harborne, J. B. (1998). Phytochemical methods: A guide to modern techniques of plant analysis (3rd ed.). Springer.

Iravani, S. (2011). Green synthesis of metal nanoparticles using plants. Green Chemistry, 13(10), 2638-2650. https://doi.org/10.1039/C1GC15386B

Ismail, R. A., Mustafa, M. A., Ali, M. A., Jaber, A. A., & Alwahib, A. H. (2022). Antimicrobial applications of green synthesized bimetallic nanoparticles: A review. Frontiers in Chemistry, 10, 1049495. https://doi.org/10.3389/fchem.2022.1049495

Lewis, K. (2010). Persister cells. Annual Review of Microbiology, 64, 357-372. https://doi.org/10.1146/annurev.micro.112408.134306

Mujeeb, A. A., Khan, N. A., Jamal, F., Alam, K. F. B., Saeed, H., Kazmi, S., Alshameri, A. W. F., Kashif, M., Ghazi, I. A., & Owais, M. (2020). Olax scandens mediated biogenic synthesis of Ag-Cu nanocomposites: Potential against inhibition of drug-resistant microbes. Frontiers in Chemistry, 8, 103. https://doi.org/10.3389/fchem.2020.00103

Nordmann, P., Poirel, L., Toleman, M. A., & Walsh, T. R. (2011). Carbapenem resistance mediated by plasmid-determined NDM-1. Journal of Antimicrobial Chemotherapy, 66(12), 2720-2721. https://doi.org/10.1093/jac/dkr397

O'Neill, J. (2016). Tackling drug-resistant infections globally: Final report and recommendations. Review on Antimicrobial Resistance.

O'Toole, G. A. (2011). Microtiter dish biofilm formation assay. Journal of Visualized Experiments, 47, e2437. https://doi.org/10.3791/2437

Padilla-Cruz, A. L., Garza-Cervantes, J. A., Vasto-Anzaldo, X. G., Garcia-Rivas, G., Leon-Buitimea, A., & Morones-Ramirez, J. R. (2021). Synthesis and design of Ag-Fe bimetallic nanoparticles as antimicrobial agents using Gardenia jasminoides leaf extract. Scientific Reports, 11, 4921. https://doi.org/10.1038/s41598-021-84768-8

Ragavendran, C., Kamaraj, C., Natarajan, D., Al-Ghanim, K. A., Magesh, M., Nicoletti, M., & Govindarajan, M. (2024). Synthesis of Lawsonia inermis-encased silver-copper bimetallic nanoparticles with antioxidant, antibacterial, and cytotoxic activity. Green Processing and Synthesis, 13, 20230194. https://doi.org/10.1515/gps-2023-0194

Sani, I., Ukwuani-Kwaja, A. N., & Abdulkadir, D. (2022). Antibacterial activities of plant-derived metallic nanoparticles on some selected multidrug-resistant clinical isolates. Asian Journal of Biological Sciences, 15, 15-26. https://doi.org/10.3923/ajbs.2022.15.26

Singleton, V. L., & Rossi, J. A. (1965). Colorimetry of total phenolics with phosphomolybdic-phosphotungstic acid reagents. American Journal of Enology and Viticulture, 16(3), 144-158.

Slavin, Y. N., Asnis, J., Hafeli, U. O., & Bach, H. (2017). Metal nanoparticles: Understanding the mechanisms behind antibacterial activity. Journal of Nanobiotechnology, 15, 65. https://doi.org/10.1186/s12951-017-0308-z

World Health Organization. (2024). WHO bacterial priority pathogens list, 2024: Bacterial pathogens of public health importance to guide research, development and strategies to prevent and control antimicrobial resistance. WHO.

Cite this article as: *Bansal P and Sethi N. Green Synthesis and Antibacterial Activity of Fittonia albivenis-Mediated CuO–Ag Nanoparticles. Int. J. Sci. Info. March, 2025, 2(12), 21-34*

Source of support: Nil, Conflict of interest: None Declared